

# Antigenic assessment of the H3N2 component of the 2019-2020 Northern Hemisphere influenza vaccine

Sigrid Gouma<sup>1</sup>, Madison Weirick<sup>1</sup> & Scott E. Hensley<sup>1</sup>✉

The 2019–2020 Northern Hemisphere influenza vaccine includes antigens from 3c3.A H3N2 viruses; however, over half of circulating H3N2 viruses belong to subclade 3c2.A1b. Here, we analyze antibody responses elicited by the egg-adapted 3c3.A H3N2 vaccine strain in ferrets and humans. We find that this vaccine strain elicits antibodies that have reduced reactivity to a wild-type 3c3.A strain and very limited reactivity to 3c2.A strains, including the currently circulating 3c2.A1b strain.

<sup>1</sup>Department of Microbiology, Perelman School of Medicine, University of Pennsylvania, Philadelphia, PA, USA. ✉email: [hensley@penmedicine.upenn.edu](mailto:hensley@penmedicine.upenn.edu)

**H**3N2 influenza viruses include many subclades with different genetic and antigenic properties<sup>1</sup>. Antigenically distinct 3c2.A and 3c3.A H3N2 viruses emerged during the 2014–2015 season<sup>2</sup>, which led to a major vaccine mismatch and low vaccine effectiveness<sup>3,4</sup>. 3c2.A H3N2 viruses have predominated since then and antigens from these viruses have been included in vaccine formulations for the 2015–2016 to 2018–2019 seasons<sup>1,5</sup>. 3c2.A H3N2-based vaccines have been relatively ineffective<sup>4</sup>, partly because the hemagglutinins (HAs) of these viruses lose an antigenically important glycosylation site when propagated in eggs during the vaccine production process<sup>6</sup>. 3c3.A H3N2 viruses have circulated at low levels since the 2014–2015 season but unexpectedly dominated circulation in the United States during the late part of the 2018–2019 US influenza season<sup>1,7</sup>. Due to the unexpected late circulation of 3c3.A H3N2 viruses, the World Health Organization (WHO) postponed their recommendation of 2019–2020 H3N2 vaccine strains during their vaccine strain selection meeting in February of 2019. A month later, the WHO recommended that antigens from 3c3.A H3N2 viruses should be included in the 2019–2020 formulation<sup>7</sup>. This was a controversial decision at the time, as 3c2.A H3N2 viruses were circulating at high levels in most places in the world other than the United States<sup>8</sup>. So far, very low levels of H3N2 viruses have circulated in the United States over the course of the 2019–2020 Northern Hemisphere influenza season<sup>9</sup>; however, H3N2 virus activity has been elevated in other parts of the world<sup>10</sup>. There has been significant diversity among currently circulating H3N2 viruses. For example, in Europe only 42% of sequenced H3N2 viruses from the 2019–2020 influenza season belong to the 3c3.A clade, whereas 58% belong to the 3c2.A clade<sup>11</sup>.

Given the heterogeneity among circulating H3N2 viruses, we completed a series of experiments to assess the antigenic characteristics of the current 3c3.A H3N2 vaccine strain. Using antibodies elicited in ferrets and humans, we find that the H3N2 component of the 2019–2020 Northern Hemisphere influenza vaccine is antigenically mismatched to most circulating H3N2 viral strains.

## Results

**Antigenicity of the egg-adapted 3c3.A vaccine strain.** First, we analyzed antibodies from ferrets infected with either the egg-adapted A/Kansas/14/2017 3c3.A H3N2 vaccine strain or the wild-type A/Kansas/14/2017 3c3.A H3N2 virus. We tested antibodies raised against both wild-type and egg-adapted viruses, because egg adaptations can affect the antigenic properties of influenza vaccine strains<sup>6,12</sup>. The HAs of these two viruses differ by only three amino acids (Fig. 1a). Ferrets infected with the wild-type 3c3.A strain produced antibodies that neutralized wild-type and egg-adapted 3c3.A viruses equivalently, whereas ferrets infected with the egg-adapted 3c3.A strain mounted antibody responses that efficiently neutralized egg-adapted 3c3.A virus and only moderately neutralized wild-type 3c3.A virus (Fig. 1b, c). We used reverse genetics to introduce each egg-adaptive HA substitution into wild-type 3c3.A viruses to determine which substitutions were responsible for the antigenic differences between the egg-adapted and wild-type viruses. The introduction of the egg-adapted G186V and D190N substitutions into the HA of wild-type 3c3.A viruses increased reactivity of antibodies elicited by the egg-adapted 3c3.A virus (Fig. 1c). Both of these substitutions are located in antigenic site B (Fig. 1a), indicating that 3c3.A viruses elicit an antibody response that is biased towards HA antigenic site B in ferrets.

**Ferret antibodies are focused towards HA antigenic site B.** HA antigenic site B of 3c3.A and 3c2.A H3N2 viruses are distinct, as 3c3.A viruses possess K160 and 3c2.A viruses possess T160, which

results in the introduction of a glycosylation site<sup>6</sup> at HA residue 158 (Fig. 1a). We therefore tested reactivity of the ferret antibodies to a panel of 3c2.A viruses, including a 3c2.A1b isolate that is representative of currently circulating 3c2.A H3N2 strains (Fig. 1d, e). Antibodies from ferrets exposed to the wild-type or egg-adapted 3c3.A strain reacted poorly to all 3c2.A H3N2 viruses tested (Fig. 1d, e). We used reverse genetics to engraft HA site A or B from 3c2.A viruses onto 3c3.A viruses and HA site A or B from 3c3.A viruses onto 3c2.A viruses. Antibodies from ferrets exposed to the wild-type or egg-adapted 3c3.A strain reacted more efficiently to viruses that possessed HA site B from 3c3.A viruses (Fig. 1d, e), confirming that 3c3.A H3N2 elicits primarily an HA antigenic site B-focused response that fails to recognize 3c2.A HA.

## Human antibodies are focused towards HA antigenic site B.

Studies from our laboratory and others have demonstrated that ferrets and humans can have different anti-influenza virus antibody specificities, because most humans have extensive influenza virus immune histories<sup>13</sup>. We therefore analyzed serum antibodies collected from 62 humans before and after vaccination with an egg-based 2019–2020 Northern Hemisphere influenza vaccine. The median age of the participants in our study was 34 years (range 18–66 years) and 44 participants (71%) were female. Fifty-seven participants (92%) reported that they received at least one influenza vaccine during the last 2 years. Pre-vaccination antibody titers to wild-type 3c3.A virus, egg-adapted 3c3.A virus, and 3c2.A virus were low in most participants (Fig. 2a). After vaccination, antibody titers to all viruses increased (Fig. 2a–c), but titers against the egg-adapted 3c3.A strain were higher (geometric mean titer (GMT) 209; 95% confidence interval (CI) 156–281) compared with titers against the wild-type 3c3.A strain (GMT 78; 95% CI 58–104) and the 3c2.A1b strain (GMT 25; 95% CI 19–33) (Fig. 2a). We found that 60 out of 62 participants (97%) had detectable antibody titers to the 3c3.A H3N2 vaccine strain after vaccination, whereas only 35 out of 62 participants (56%) had detectable neutralizing antibody titers to 3c2.A1b H3N2 (Fig. 2a). We also tested 3c3.A viruses that were engineered to possess either HA site A or site B from 3c2.A viruses (Fig. 2a, b, blue and red, respectively). Antibodies elicited by the vaccine reacted poorer to 3c3.A virus that possessed HA antigenic site B from 3c2.A viruses (Fig. 2a, b), indicating that the vaccine mismatch between 3c3.A and 3c2.A viruses is primarily due to differences in HA antigenic site B.

## Discussion

Our within-season antigenic analyses indicate that the 3c3.A H3N2 component of the 2019–2020 Northern Hemisphere influenza vaccine strain is antigenically distinct compared with circulating 3c2.A H3N2 viruses. It will be important to continually monitor the frequencies of 3c3.A vs. 3c2.A H3N2 viruses, as it is not clear whether one of these antigenically distinct H3N2 clades will predominate future influenza seasons, and therefore it will be difficult to make H3N2 component recommendations for future influenza vaccines. Ideally, antigens from both 3c3.A and 3c2.A H3N2 viruses will be included in future influenza vaccines; however, there are practical considerations that might not allow that to be immediately feasible. It is interesting that the community-based Canadian Sentinel Practitioner Surveillance Network recently reported interim 2019–2020 H3N2 vaccine effectiveness estimates that are relatively high, despite the observation that the majority of H3N2 viruses that circulated in Canada over the past year are not within the 3c3.A clade<sup>14</sup>. Additional studies analyzing vaccine effectiveness against specific 3c3.A and 3c2.A H3N2 viral strains will be important to better understand these interim findings from Canada.

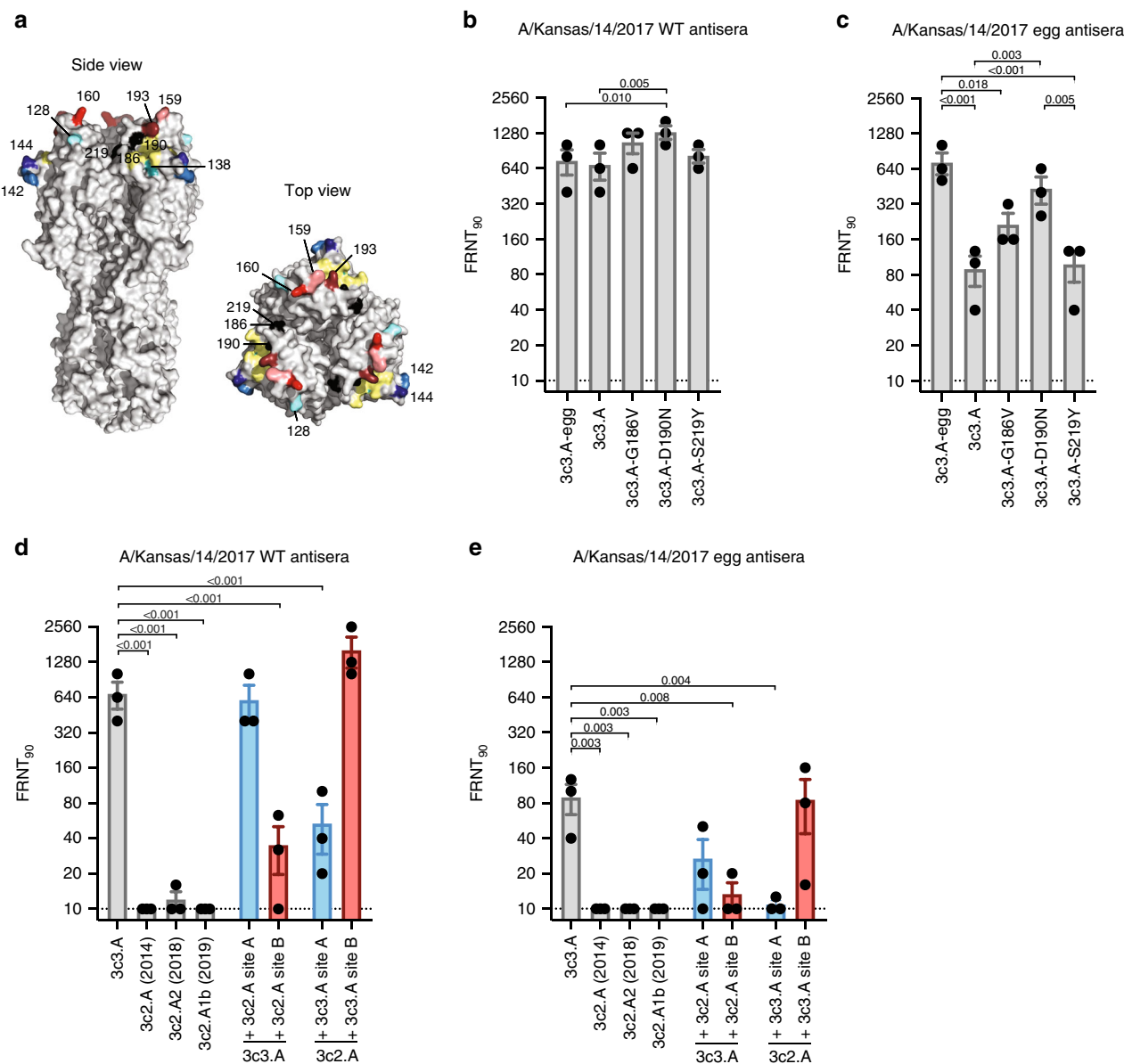


**Fig. 1** Antigenic mismatch of the H3N2 component of the 2019–2020 Northern Hemisphere influenza vaccine. **a** Crystal structure of the HA trimer of A/Victoria/361/2011 (PDB accession code 4O51) with the amino acid substitutions that differ between egg-adapted and wild-type A/Kansas/14/2017 (positions 186, 190, and 219) shown in black and the amino acid substitutions that differ between wild-type A/Kansas/14/2017 and other 3c2.A H3N2 subclades in antigenic sites A (positions 128, 138, 142, and 144) and B (positions 159, 160, and 193) shown in blue and red, respectively. The receptor-binding pocket is indicated in yellow. **b** Neutralizing antibody titers (FRNT<sub>90</sub>) to wild-type A/Kansas/14/2017 (3c3.A) and egg-adapted A/Kansas/14/2017 (3c3.A-egg) using wild-type A/Kansas/14/2017 antisera ( $n = 3$  ferrets, each data point represents the geometric mean titer from three independent experiments). Data are presented as mean  $\pm$  SEM. Log<sub>2</sub>-transformed antibody titers were compared using RM one-way ANOVA corrected for multiple comparisons (Bonferroni method).  $P$ -values  $< 0.05$  are indicated. **c** Neutralizing antibody titers (FRNT<sub>90</sub>) to wild-type A/Kansas/14/2017 (3c3.A) and egg-adapted A/Kansas/14/2017 (3c3.A-egg) using egg-adapted A/Kansas/14/2017 antisera ( $n = 3$  ferrets, each data point represents the geometric mean titer from three independent experiments). Data are presented as mean  $\pm$  SEM. Log<sub>2</sub>-transformed antibody titers were compared using RM one-way ANOVA corrected for multiple comparisons (Bonferroni method).  $P$ -values  $< 0.05$  are indicated. **d, e** Neutralizing antibody titers (FRNT<sub>90</sub>) to a panel of H3N2 viruses using wild-type A/Kansas/14/2017 and egg-adapted A/Kansas/14/2017 antisera ( $n = 3$  ferrets per group, each data point represents the geometric mean titer from three independent experiments). 3c3.A virus with 3c2.A site A possesses amino acid substitutions A128T, S138A, G142R, and K144S. 3c3.A virus with 3c2.A site B possesses amino acid substitutions S159Y, K160T, and S193F. 3c2.A virus with 3c3.A site A possesses amino acid substitutions T128A, A138S, R142G, and S144K. 3c2.A virus with 3c3.A site B possesses amino acid substitutions Y159S, T160K, and F193S. Data are presented as mean  $\pm$  SEM. Log<sub>2</sub>-transformed antibody titers were compared using RM one-way ANOVA corrected for multiple comparisons (Bonferroni method). Significant differences relative to 3c3.A are indicated ( $p < 0.05$ ). Source data are provided as a Source Data file.

**Methods**

**Viruses.** We used reverse genetics<sup>3</sup> to create viruses for this study. For ferret infections, we created 3c3.A viruses with the wild-type or egg-adapted A/Kansas/14/2017 HA (GISAID accession numbers EPI1146345 and EPI1144535). The egg-adapted HA possessed amino acid substitutions G186V, D190N, and S219Y relative to the wild-

type HA (Fig. 1a). All 3c3.A viruses were rescued using wild-type A/Kansas/14/2017 NA (GISAID accession number EPI1146344). Other viruses in our panel included HAs from A/Colorado/15/2014 (3c2.A, GISAID accession number EPI545672), A/North Carolina/28/2019 (3c2.A1b, GISAID accession number EPI1606044), or A/Pennsylvania/49/2018 (3c2.A2, GISAID accession number EPI1197412). NA from A/

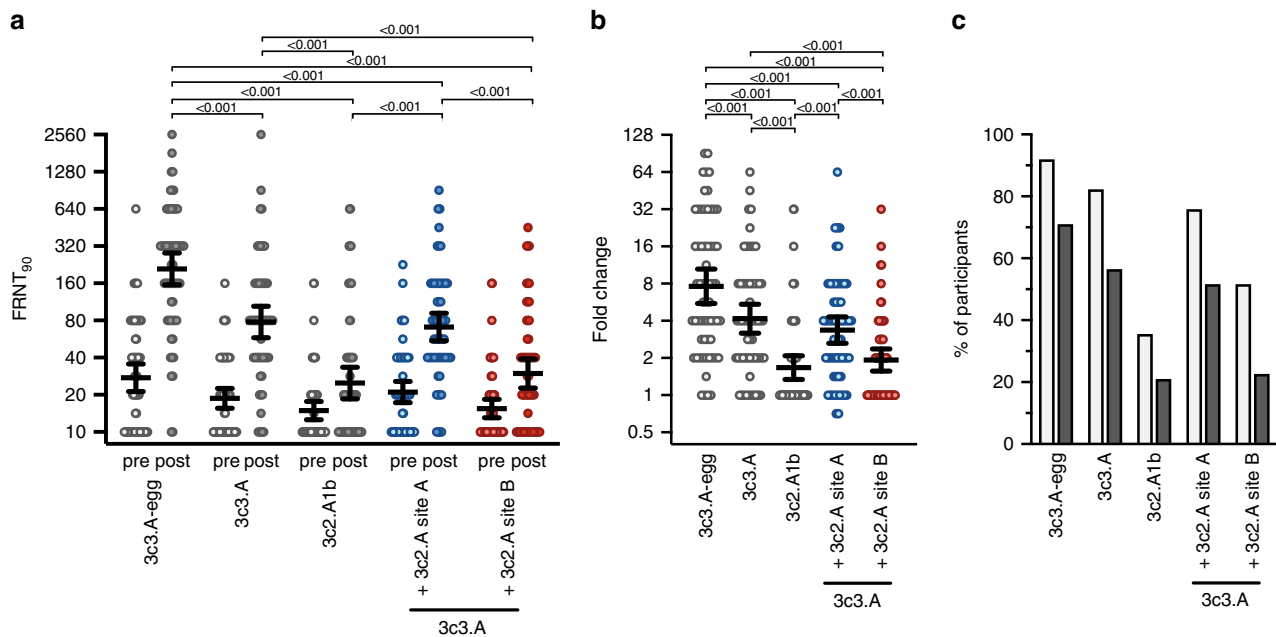


**Fig. 2 Neutralizing antibody titers (FRNT<sub>90</sub>) to a panel of H3N2 viruses in sera from adults ( $n = 62$ ) who received the 2019–2020 Northern Hemisphere influenza vaccine. **a** Pre- and post-vaccination titers. Each data point represents the geometric mean titer from two independent experiments. Thick horizontal lines show the geometric means and error bars indicate the 95% confidence intervals. Log<sub>2</sub>-transformed antibody titers were compared using RM one-way ANOVA corrected for multiple comparisons (Bonferroni method).  $P$ -values  $< 0.05$  are indicated. **b** Fold change of geometric mean neutralizing antibody titers (FRNT<sub>90</sub>) upon vaccination. Post-vaccination titers were divided by pre-vaccination titers to calculate fold change. Thick horizontal lines show the geometric means and error bars indicate the 95% confidence intervals. Log<sub>2</sub>-transformed antibody titers were compared using RM one-way ANOVA corrected for multiple comparisons (Bonferroni method).  $P$ -values  $< 0.05$  are indicated. **c** Seroconversion rates upon vaccination. Light gray bars indicate at least a twofold increase in antibody titer. Dark gray bars indicate at least a fourfold increase in antibody titer. 3c3.A virus with 3c2.A site A possesses amino acid substitutions A128T, S138A, G142R, and K144S. 3c3.A virus with 3c2.A site B possesses amino acid substitutions S159Y, K160T, and S193F. Source data are provided as a Source Data file.**

North Carolina/28/2019 (GISAID accession number EPI1606043) was used to create 3c2.A1b virus and NA from A/Colorado/15/2014 (3c2.A, GISAID accession number EPI545672) was used to create 3c2.A and 3c2.A2 viruses. Mutant viruses were created using either wild-type A/Kansas/14/2017 (3c3.A) or A/Colorado/15/2014 (3c2.A) HA as a backbone. 3c3.A virus with 3c2.A HA site A possesses HA amino acid substitutions A128T, S138A, G142R, and K144S. 3c2.A virus with 3c3.A HA site A possesses HA amino acid substitutions T128A, A138S, R142G, and S144K. 3c3.A virus with 3c2.A HA site B possesses HA amino acid substitutions S159Y, K160T, and S193F. 3c2.A virus with 3c3.A HA site B possesses HA amino acid substitutions Y159S, T160K, and F193S. All viruses were rescued using A/Puerto Rico/8/1934 internal genes to allow efficient viral growth in culture.

**Ferret sera.** Ferrets were infected with 200,000 foci-forming units (FFUs) of virus with either wild-type A/Kansas/14/2017 ( $n = 3$ ) or egg-adapted A/Kansas/14/2017 ( $n = 3$ ) HA, and then bled 28 days later. Ferrets tested negative for influenza-specific antibodies in enzyme-linked immunosorbent assay prior to infection. All animal experiments were completed under an Institutional Animal Care and Use Committee-approved protocol at Noble Life Sciences (Gaithersburg, MD).

**Human sera.** Paired serum samples were collected from 62 participants at the University of Pennsylvania 1–12 days before and 26–33 days after vaccination in October 2019 with the 2019–2020 Northern Hemisphere influenza vaccine. All participants received either Fluarix ( $n = 60$ ) or Fluzone ( $n = 2$ ), which are both quadrivalent egg-based vaccines. Informed consent was obtained from all participants. The study was approved by the institutional review board of the University of Pennsylvania.

**Foci reduction neutralization tests.** Serum samples were treated with receptor-destroying enzyme (RDE) (Denka Seiken) followed by heat-inactivation at 55 °C for 30 min prior to testing in foci reduction neutralization tests (FRNTs). RDE-treated serum samples were serially diluted in twofold and ~300 FFUs of virus were added to each diluted serum sample in a 96-well plate. Plates were incubated for 1 h at room temperature before 100  $\mu$ L of virus–serum mixtures were added to each well in a 96-well plate with confluent monolayers of MDCK-SIAT1 cells. After 1 h incubation at 37 °C in 5% CO<sub>2</sub>, cells were washed and an overlay of 1.25% Avicel in Minimal Essential Media (Gibco) supplemented with 0.2% gentamicin and 1% 1 M 4-(2-

hydroxyethyl-1-piperazineethanesulfonic acid (Gibco) was added to the cells. Cells were incubated for 18 h at 37 °C in 5% CO<sub>2</sub> and then fixed with 4% paraformaldehyde for 1 h at 4 °C. Cells were lysed with 0.5% Triton X-100 in phosphate-buffered saline (PBS) for 7 min and blocked with 5% milk in PBS for 1 h at room temperature. Plates were washed and 50  $\mu$ L of anti-nucleoprotein monoclonal antibody IC5-1B7 (BEI) 1:5000 diluted in 5% milk in PBS was added to each well. Plates were incubated for 1 h at room temperature and washed before 50  $\mu$ L of anti-mouse peroxidase-conjugated secondary antibody (Fisher) 1:1000 diluted in 5% milk in PBS was added to each well. After incubation for 1 h at room temperature, plates were washed and 3,3',5,5'-tetramethylbenzidine substrate (Kirkegaard & Perry Laboratories) was added for visualization of the foci. An ELISpot reader was used for imaging and quantification of foci. FRNT<sub>90</sub> titers are reported as the reciprocal of the highest dilution of sera that reduced the number of foci by at least 90%, relative to control wells that had no serum added. An anti-A-Colorado/15/2014 polyclonal serum in-house control was included in each assay run. Serum samples with a reduction of  $< 90\%$  in the number of foci at a 1:20 dilution were assigned an FRNT<sub>90</sub> titer of 10. Each ferret sample was tested in three independent experiments and each human sera was tested in two independent experiments. Geometric mean titers of the replicates were used for analysis.

**Statistical methods.** Log<sub>2</sub>-transformed antibody titers measured in ferret and human sera were compared using repeated-measures one-way analysis of variance corrected for multiple comparisons (Bonferroni method). Statistical analysis was performed using Prism version 8 (GraphPad Software) and R version 3.5.3 (R Foundation for Statistical Computing).

**Reporting summary.** Further information on research design is available in the Nature Research Reporting Summary linked to this article.

### Data availability

Source data for Figs. 1b–e and 2 are provided in the Source Data file. The crystal structure of the HA trimer of A/Victoria/361/2011 is available via the Protein Data Bank (PDB accession code 4O51).

Received: 15 March 2020; Accepted: 19 April 2020;  
Published online: 15 May 2020

## References

1. Jorquera, P. A. et al. Insights into the antigenic advancement of influenza A (H3N2) viruses, 2011–2018. *Sci. Rep.* **9**, 2676 (2019).
2. Yokoyama, M. et al. Molecular dynamics simulation of the influenza A(H3N2) hemagglutinin trimer reveals the structural basis for adaptive evolution of the recent epidemic clade 3C.2a. *Front. Microbiol.* **8**, 584 (2017).
3. Chambers, B. S., Parkhouse, K., Ross, T. M., Alby, K. & Hensley, S. E. Identification of hemagglutinin residues responsible for H3N2 antigenic drift during the 2014–2015 influenza season. *Cell Rep.* **12**, 1–6 (2015).
4. CDC. Past seasons vaccine effectiveness estimates. <https://www.cdc.gov/flu/vaccines-work/past-seasons-estimates.html>. Accessed 2 May 2020.
5. Garten, R. et al. Update: influenza activity in the United States during the 2017–18 season and composition of the 2018–19 influenza vaccine. *MMWR Morb. Mortal. Wkly Rep.* **67**, 634–642 (2018).
6. Zost, S. J. et al. Contemporary H3N2 influenza viruses have a glycosylation site that alters binding of antibodies elicited by egg-adapted vaccine strains. *Proc. Natl Acad. Sci. USA* **114**, 12578–12583 (2017).
7. WHO. Addendum to the recommended composition of influenza virus vaccines for use in the 2019–2020 northern hemisphere influenza season. [https://www.who.int/influenza/vaccines/virus/recommendations/201902\\_recommendation\\_addendum.pdf](https://www.who.int/influenza/vaccines/virus/recommendations/201902_recommendation_addendum.pdf). Accessed 2 May 2020.
8. Bedford, T., Huddleston, J., Potter, B. & Neher, R.A. Seasonal influenza circulation patterns and projections for September 2019 to September 2020. Preprint at <https://www.biorxiv.org/content/10.1101/780627v2> (2019).
9. CDC. Weekly U.S. influenza surveillance report. <https://www.cdc.gov/flu/weekly/index.htm>. Accessed 2 May 2020.
10. ECDC. Influenza virus characterisation, summary Europe, December 2019. <https://www.ecdc.europa.eu/en/publications-data/influenza-virus-characterisation-december-2019>. Accessed 2 May 2020.
11. ECDC-WHO/Europe. Flu news Europe. <https://flunews europe.org>. Accessed 2 May 2020.
12. Wu, N. C. et al. A structural explanation for the low effectiveness of the seasonal influenza H3N2 vaccine. *PLoS Pathog.* **13**, e1006682 (2017).
13. Cobey, S. & Hensley, S. E. Immune history and influenza virus susceptibility. *Curr. Opin. Virol.* **22**, 105–111 (2017).
14. Skowronski, D.M., et al. Interim estimates of 2019/20 vaccine effectiveness during early-season co-circulation of influenza A and B viruses, Canada, February 2020. *Euro Surveill* **25**, 2000103 (2020).

## Acknowledgements

This work was funded by institutional funds from the University of Pennsylvania and the National Institute of Allergy and Infectious Diseases at the National Institutes of Health (R01AI113047 (S.E.H.), R01AI108686 (S.E.H.), and HHSN272201400005C

(S.E.H.). S.E.H. holds an Investigators in the Pathogenesis of Infectious Disease Awards from the Burroughs Wellcome Fund. We thank the participants that took part in this study and the Penn Center for Human Phenomic Science unit for assisting in human blood draws.

## Author contributions

S.G. and S.E.H. designed the study. S.G. and M.W. completed experiments. S.G. and S.E.H. analyzed data and wrote the manuscript.

## Competing interests

S.E.H. reports receiving consulting fees from Sanofi Pasteur, Lumen, Novavax, and Merck. S.G. and M.W. declare no competing interests.

## Additional information

**Supplementary information** is available for this paper at <https://doi.org/10.1038/s41467-020-16183-y>.

**Correspondence** and requests for materials should be addressed to S.E.H.

**Peer review information** *Nature Communications* thanks the anonymous reviewers for their contribution to the peer review of this work. Peer reviewers are available.

**Reprints and permission information** is available at <http://www.nature.com/reprints>

**Publisher's note** Springer Nature remains neutral with regard to jurisdictional claims in published maps and institutional affiliations.



**Open Access** This article is licensed under a Creative Commons Attribution 4.0 International License, which permits use, sharing, adaptation, distribution and reproduction in any medium or format, as long as you give appropriate credit to the original author(s) and the source, provide a link to the Creative Commons license, and indicate if changes were made. The images or other third party material in this article are included in the article's Creative Commons license, unless indicated otherwise in a credit line to the material. If material is not included in the article's Creative Commons license and your intended use is not permitted by statutory regulation or exceeds the permitted use, you will need to obtain permission directly from the copyright holder. To view a copy of this license, visit <http://creativecommons.org/licenses/by/4.0/>.

© The Author(s) 2020